The technique that constructs strain ellipsoid from three strain ellipses measured on non-parallel sections based on the least square method and the factors that control precision of strain

Bull. Fac. Sci., Univ. Ryukyus, No.71 : 47 – 70 (2001)

The technique that constructs strain ellipsoid from three strain ellipses measured on non-parallel sections based on the least square method and the factors that control precision of strain

Daigoro HAYASHI*

Abstract

The least square strain technique that was developed by Hayashi (1994) and is based on the least square method is explained in detail. The technique uses the strain ellipses on three non-parallel section planes of oriented rock samples to construct strain ellipsoid. Three series of model are prepared to examine what kind of factor controls the precision of strain where the axial ratio of initial strain marker ellipsoids is assumed to scatter as normal distribution. Three series of model are produced to test three factors; (1) The sample size of markers. (2) The mean of axial ratio of makers and (3) The standard deviation of axial ratio of markers. Results of the simulation are; (1) When the sample size of the initial strain marker ellipsoids is large, higher the precision of strain analysis is. (2) When the mean of axial ratio of the initial strain marker ellipsoids is small, higher the precision of strain analysis is. (3) Although the standard deviation of axial ratio of the initial strain marker ellipsoids varies, the precision of strain analysis does not change.

1. Introduction

There are several techniques that are developed to construct strain ellipsoid by using strain ellipses on three section planes. The techniques that construct strain ellipsoid using strain ellipses on three mutually perpendicular planes, were described by Ramsay(1967), Oertel(1970), Roberts and Siddans(1971) and Shimamoto and Ikeda(1976). Since the strain ellipse that is measured on a section plane includes error, the shape of the strain ellipse does not coincide the projection of strain ellipsoid to the plane. We can theoretically obtain six strain ellipsoids from the three measured strain ellipses (Hayashi;1994,1995). If the measurement of the three strain ellipses does not include error, the six strain ellipsoids equal to each other. Thus the techniques that use the strain ellipses on the mutually perpendicular planes are derived from the idea. The shape tensor of the strain ellipsoid is given as the mean of the shape tensor of the six strain ellipsoids. Thus we agree that the strain ellipses that we will measure, do not necessarily lie on mutually perpendicular planes.

*Department of Physics and Earth Sciences, University of the Ryukyus,Nishihara, Okinawa, 903-0213, Japan e-mail:daigoro@sci.u-ryukyu.ac.jp fax 098-895-8552

From the point of view, Milton(1980), Owens(1984), De Paor(1990) and Hayashi(1994) have developed the methods that construct strain ellipsoid using strain ellipses on non-parallel planes by means of the least square method except for Milton. Although Hayashi(1994) has described the technique of three dimensional strain analysis based on the least square method in detail, he has not examined the precision of the technique.

In the present paper I have explained the strain analysis technique that was developed by Hayashi (1994). The technique is called here "least square strain technique". Then I have simulated three series of strain analysis to examine the relation between the precision of the least square strain analysis and the three factors. The shape of the strain markers is assumed to be ellipsoid. Their axial ratio $R_i(=\frac{X_i}{Z_i})$ is supposed to show normal distribution. Three factors are (1) the variation of sample size of strain markers, (2) the variation of mean of the axial ratio (R_i) of strain markers and (3) the variation of standard deviation of the axial ratio (R_i) of strain markers. The simulation is performed as follows. (1) Several hundred randomly oriented marker ellipsoids are produced. (2) They are deformed to have (R_f, ϕ) data. (3) Strain ellipsoid is calculated using the (R_f, ϕ) data by means of the least square strain technique.

2. Least square strain technique

2.1 Two dimensional strain analysis

The methods how to obtain strain ellipse using marker ellipses on each non-parallel plane, that is, the techniques of two dimensional strain analysis were developed by many researchers. The techniques of two dimensional strain analysis are divided into two categories. One is the shape method where we treat strain markers as if their shape is ellipse, and the other is the direction method where we use any suitable lines, for example, mineral grain boundary, as a strain marker. The shape methods were described by Ramsay(1967), Dunnet(1969), Elliott(1970), Dunnet and Siddans(1971), Matthews et al. (1974), Shimamoto and Ikeda(1976) and Lisle(1977,1985). The direction methods were published by Sanderson(1977), Fry(1979) and Panozzo(1984). We can use one of them to obtain strain ellipse on a section plane of oriented rock samples.

2.2 GS method

When we want to construct strain ellipsoid using strain ellipses on mutually non-parallel planes, we should describe the long and short axial length of the strain ellipses on non-parallel planes by the ratio of axial length assuming a certain axial length of a certain strain ellipse to be unity. To do this, I have used the method developed by Gendzwill and Stauffer(1981). The method is called here "GS method". The method was originally developed in order to calculate the ellipse on the plane that includes the center of the ellipsoid, if a given ellipse lies on a plane that does not include the center of an ellipsoid. I have used the GS method to obtain relative axial length of ellipses on mutually non-parallel plane sections.

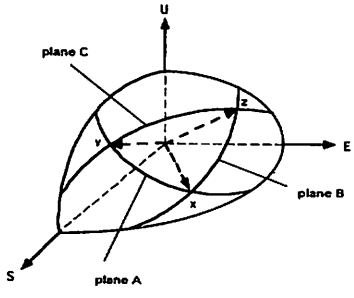

Fig.1 Strain ellipsoid shown in SEU-coordinate system. Three planes A, B and C that include the center of the ellipsoid are arbitrarily cut. Three vectors x, y and are the intersecting lines of two planes among the three planes.

As shown in Fig.1, let cut arbitrarily an ellipsoid through

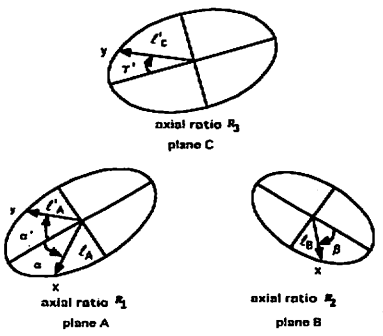

Fig.2 Strain ellipse on three planes A, B and C. See text for detail.

three section planes A, B and C that include the center of the ellipsoid, and let define the intersecting line between A and B as vector **x** . The elongation along vector **x** on both planes A and B must be equal. If the plane A does not include the center of the ellipsoid, the shape of the ellipse on the plane A is similar but its area is constricted than that of the ellipse on the plane. The plane is parallel to A and passes through the center of the ellipsoid.

As shown on the plane A in Fig.2, considering the length of **x** as l_A, the point $(l_A \cos\alpha,\ l_A \sin\alpha)$ is a tip point of **x** in the coordinate system where the long axis and the short axis of the ellipse are taken as abscissa and ordinate, respectively. Since the tip point lies on the arc of the ellipse, supposing the axial ratio of the strain ellipse on the plane A to be R_1 , the tip point satisfies the relation

$$\left(\frac{x}{R_1}\right)^2 + y^2 = 1$$

Then we have

$$\frac{l_A^2 \cos^2\alpha}{R_1^2} + l_A^2 \sin^2\alpha = 1.$$

This is modified to

$$\frac{1}{l_A^2} = 1 - \left(1 - \frac{1}{R_1^2}\right) \cos^2\alpha .$$

For the case of plane B, considering the length of **x** to be l_B and the strain ratio on B to be R_2, we have

$$\frac{1}{l_B^2} = 1 - \left(1 - \frac{1}{R_2^2}\right) \cos^2\beta .$$

The section multiplier p of the plane A to the plane B is obtained from $l_A = p l_B$ as $p = \frac{l_A}{l_B}$.

I have taken the same approach described above to estimate the section multiplier q of the plane C to the plane A. Suppose that (1) the intersecting line of the planes A and C is vector **y** , (2) on the plane A the length of **y** is l_A' (3) on the plane A the angle between long axis of strain ellipse and **y** is α', (4) on the plane C the length of **y** is l_C' (5) on the plane C the angle between long axis of strain ellipse and **y** is γ' , and (6) the strain ratio is R_3 on the plane C. Then the section multiplier q of the plane C to the plane A is obtained from the relation

$$l_A' = q l_C' \quad as \quad q = \frac{l_A'}{l_C'} \text{ where}$$

$$\frac{1}{l_A'^2} = 1 - \left(1 - \frac{1}{R_1^2}\right) \cos^2\alpha'.$$

$$\frac{1}{l_C'^2} = 1 - \left(1 - \frac{1}{R_3^2}\right) \cos^2\gamma'.$$

Supposing the length of the short axis on the plane A to be unity, we have relative length of the long and short axial length on all the planes as (1) $X=R_1$ and $Y=1$ for the plane A, (2) $X=R_2p$ and $Y=p$ for the plane B and (3) $X=R_3q$ and $Y=q$ for the plane C.Thus the GS method can be used to calculate relative axial length on the section planes by using the section multipliers p and q.

Incidentally relative principal reciprocal quadratic extensions λ_1' and λ_2' are written according to their definition as $\lambda_1' = \frac{1}{\lambda_1} = \frac{1}{X^2}$ and $\lambda_2' = \frac{1}{\lambda_2} = \frac{1}{Y^2}$, respectively.

2.3 Least square strain technique

The least square strain technique that extrapolates strain ellipsoid using the relative axial length of strain ellipses on mutually non-parallel planes, is explained as follows. Any ellipsoid is written as

$$ax^2 + 2bxy + 2czx + dy^2 + 2eyz + hz^2 = 1.$$

Consider the next function

$$f(x,y,z;a,b,c,d,e,h) = ax^2 + 2bxy + 2czx + dy^2 + 2eyz + hz^2 - 1 = 0. \quad (1)$$

The problem that we should solve is to obtain the shape tensor

$$\begin{pmatrix} a & b & c \\ & d & e \\ sym & & h \end{pmatrix}$$

of the ellipsoid by measuring coordinate of points that are believed to consist the ellipsoid. The points are practically the points that are scattered on the arc of the strain ellipse on a section plane. To accomplish this purpose Hayashi(1994) proposed the next approach.

Supposing the measured coordinate of the points that consist the surface of the ellipsoid as (X_i, Y_i, Z_i) and the true coordinate as (x_i, y_i, z_i) where i takes from 1 to sum of the points, residuals are

$$\begin{cases} v_{xi} = X_i - x_i \\ v_{yi} = Y_i - y_i \\ v_{zi} = Z_i - z_i \end{cases}$$

The formula are changed to

$$\begin{cases} x_i = X_i - v_{xi} \\ y_i = Y_i - v_{yi} \\ z_i = Z_i - v_{zi} \end{cases} \quad (2)$$

The true value (x_i, y_i, z_i) satisfies Eq.(1)

$f(x_i, y_i, z_i ; a, b, c, d, e, h)=0$.

Supposing the approximate value of the six coefficients $a, b,..., h$ as $a', b',...,h'$ and considering $\varepsilon_a, \varepsilon_b,..., \varepsilon_h$ as error, we have

$$\begin{cases} a = a' - \varepsilon_a \\ b = b' - \varepsilon_b \\ \quad \cdots \\ \quad \cdots \\ h = h' - \varepsilon_h \end{cases} \quad (3)$$

It is worth to note that we can previously determine the six coefficients a', b',...,h' by using the coordinate (X_i, Y_i, Z_i) of six arbitrary measured points.

Substituting Eqs.(2) and (3) into Eq.(1), we have

$f(X_i-v_{xi}, Y_i-v_{yi}, Z_i-v_{zi}; a'-\varepsilon_a, b'-\varepsilon_b, c'-\varepsilon_c, d'-\varepsilon_d, e'-\varepsilon_e, h'-\varepsilon_h)=0$.

Expanding this by the Taylor expansion and abbreviating the terms that are under the second differential, we have

$$f(X_i,Y_i,Z_i;a',b',c',d',e',h')-\left(\frac{\partial f}{\partial x}\right)_{X_i\sim h'}v_{xi}-\left(\frac{\partial f}{\partial y}\right)_{X_i\sim h'}v_{yi}-\left(\frac{\partial f}{\partial z}\right)_{X_i\sim h'}v_{zi}-\left(\frac{\partial f}{\partial a}\right)_{X_i\sim h'}\varepsilon_a$$
$$-\left(\frac{\partial f}{\partial b}\right)_{X_i\sim h'}\varepsilon_b-\left(\frac{\partial f}{\partial c}\right)_{X_i\sim h'}\varepsilon_c-\left(\frac{\partial f}{\partial d}\right)_{X_i\sim h'}\varepsilon_d-\left(\frac{\partial f}{\partial e}\right)_{X_i\sim h'}\varepsilon_e-\left(\frac{\partial f}{\partial h}\right)_{X_i\sim h'}\varepsilon_h=0.$$

This is rewritten as

$$\varphi_i = f_{oi}-f_{xi}v_{xi}-f_{yi}v_{yi}-f_{zi}v_{zi}-f_{ai}\varepsilon_a-f_{bi}\varepsilon_b-f_{ci}\varepsilon_c-f_{di}\varepsilon_d-f_{ei}\varepsilon_e-f_{hi}\varepsilon_h=0 \tag{4}$$

where

$$f_{oi}=f(X_i,Y_i,Z_i;a',b',c',d',e',h')$$
$$f_{xi}=\left(\frac{\partial f}{\partial x}\right)_{X_i\sim h'};\quad f_{yi}=\left(\frac{\partial f}{\partial y}\right)_{X_i\sim h'};\quad f_{zi}=\left(\frac{\partial f}{\partial z}\right)_{X_i\sim h'}$$
$$f_{ai}=\left(\frac{\partial f}{\partial a}\right)_{X_i\sim h'};\quad f_{bi}=\left(\frac{\partial f}{\partial b}\right)_{X_i\sim h'};\quad f_{ci}=\left(\frac{\partial f}{\partial c}\right)_{X_i\sim h'} \tag{5}$$
$$f_{di}=\left(\frac{\partial f}{\partial d}\right)_{X_i\sim h'};\quad f_{ei}=\left(\frac{\partial f}{\partial e}\right)_{X_i\sim h'};\quad f_{hi}=\left(\frac{\partial f}{\partial h}\right)_{X_i\sim h'}.$$

Supposing the weight of each measurement as p_{xi} , p_{yi} and p_{zi} , "sum of weighted square residuals" S is

$$S=\sum_{i=1}^{n}\left(p_{xi}v_{xi}^2+p_{yi}v_{yi}^2+p_{zi}v_{zi}^2\right). \tag{6}$$

Thus to minimize Eq.(6) under the condition Eq.(4), we minimize

$$g=\frac{1}{2}S-\sum_{i=1}^{n}\lambda_i\varphi_i$$

using the Lagrangean multiplier λ_i . From the condition we have

$$\frac{\partial g}{\partial v_{xi}}=p_{xi}v_{xi}+\lambda_i f_{xi}=0 \tag{7.1}$$
$$\frac{\partial g}{\partial v_{yi}}=p_{yi}v_{yi}+\lambda_i f_{yi}=0 \tag{7.2}$$
$$\frac{\partial g}{\partial v_{zi}}=p_{zi}v_{zi}+\lambda_i f_{zi}=0 \tag{7.3}$$
$$\frac{\partial g}{\partial \varepsilon_a}=\sum_{i=1}^{n}\lambda_i f_{ai}=0 \tag{7.4}$$
$$\frac{\partial g}{\partial \varepsilon_b}=\sum_{i=1}^{n}\lambda_i f_{bi}=0 \tag{7.5}$$
$$\frac{\partial g}{\partial \varepsilon_c}=\sum_{i=1}^{n}\lambda_i f_{ci}=0 \tag{7.6}$$

$$\frac{\partial g}{\partial \varepsilon_d} = \sum_{i=1}^{n} \lambda_i f_{di} = 0 \tag{7.7}$$

$$\frac{\partial g}{\partial \varepsilon_e} = \sum_{i=1}^{n} \lambda_i f_{ei} = 0 \tag{7.8}$$

$$\frac{\partial g}{\partial \varepsilon_h} = \sum_{i=1}^{n} \lambda_i f_{hi} = 0. \tag{7.9}$$

Eqs. (7.1), (7.2) and (7.3) are changed into $v_{xi} = -\frac{\lambda_i f_{xi}}{p_{xi}}$, $v_{yi} = -\frac{\lambda_i f_{yi}}{p_{yi}}$, and $v_{zi} = -\frac{\lambda_i f_{zi}}{p_{zi}}$, respectively. Substituting these into Eq.(4), we have

$$f_{oi} + \left(\frac{f_{xi} f_{xi}}{p_{xi}} + \frac{f_{yi} f_{yi}}{p_{yi}} + \frac{f_{zi} f_{zi}}{p_{zi}} \right) \lambda_i - f_{ai}\varepsilon_a - f_{bi}\varepsilon_b - f_{ci}\varepsilon_c - f_{di}\varepsilon_d - f_{ei}\varepsilon_e - f_{hi}\varepsilon_h = 0. \tag{8}$$

Using the next equation

$$\frac{1}{p_{oi}} = \frac{f_{xi} f_{xi}}{p_{xi}} + \frac{f_{yi} f_{yi}}{p_{yi}} + \frac{f_{zi} f_{zi}}{p_{zi}}$$

, Eq.(8) becomes

$$\lambda_i = p_{oi}\left(f_{ai}\varepsilon_a + f_{bi}\varepsilon_b + f_{ci}\varepsilon_c + f_{di}\varepsilon_d + f_{ei}\varepsilon_e + f_{hi}\varepsilon_h - f_{oi} \right). \tag{9}$$

Substituting Eq.(9) into Eqs.(7.4) to (7.9), we have

$$\sum_{i=1}^{n} p_{oi} f_{ai} \left(f_{ai}\varepsilon_a + f_{bi}\varepsilon_b + f_{ci}\varepsilon_c + f_{di}\varepsilon_d + f_{ei}\varepsilon_e + f_{hi}\varepsilon_h - f_{oi} \right) = 0$$

$$\sum_{i=1}^{n} p_{oi} f_{bi} \left(f_{ai}\varepsilon_a + f_{bi}\varepsilon_b + f_{ci}\varepsilon_c + f_{di}\varepsilon_d + f_{ei}\varepsilon_e + f_{hi}\varepsilon_h - f_{oi} \right) = 0$$

$$\sum_{i=1}^{n} p_{oi} f_{ci} \left(f_{ai}\varepsilon_a + f_{bi}\varepsilon_b + f_{ci}\varepsilon_c + f_{di}\varepsilon_d + f_{ei}\varepsilon_e + f_{hi}\varepsilon_h - f_{oi} \right) = 0$$

$$\sum_{i=1}^{n} p_{oi} f_{di} \left(f_{ai}\varepsilon_a + f_{bi}\varepsilon_b + f_{ci}\varepsilon_c + f_{di}\varepsilon_d + f_{ei}\varepsilon_e + f_{hi}\varepsilon_h - f_{oi} \right) = 0$$

$$\sum_{i=1}^{n} p_{oi} f_{ei} \left(f_{ai}\varepsilon_a + f_{bi}\varepsilon_b + f_{ci}\varepsilon_c + f_{di}\varepsilon_d + f_{ei}\varepsilon_e + f_{hi}\varepsilon_h - f_{oi} \right) = 0$$

$$\sum_{i=1}^{n} p_{oi} f_{hi} \left(f_{ai}\varepsilon_a + f_{bi}\varepsilon_b + f_{ci}\varepsilon_c + f_{di}\varepsilon_d + f_{ei}\varepsilon_e + f_{hi}\varepsilon_h - f_{oi} \right) = 0.$$

Rearranging them regarding $\varepsilon_a, \varepsilon_b, \ldots, \varepsilon_h$, we have

$$\begin{aligned}
&[p_o f_a f_a]\varepsilon_a + [p_o f_a f_b]\varepsilon_b + [p_o f_a f_c]\varepsilon_c + [p_o f_a f_d]\varepsilon_d + [p_o f_a f_e]\varepsilon_e + [p_o f_a f_h]\varepsilon_h = [p_o f_a f_o] \\
&[p_o f_b f_a]\varepsilon_a + [p_o f_b f_b]\varepsilon_b + [p_o f_b f_c]\varepsilon_c + [p_o f_b f_d]\varepsilon_d + [p_o f_b f_e]\varepsilon_e + [p_o f_b f_h]\varepsilon_h = [p_o f_b f_o] \\
&[p_o f_c f_a]\varepsilon_a + [p_o f_c f_b]\varepsilon_b + [p_o f_c f_c]\varepsilon_c + [p_o f_c f_d]\varepsilon_d + [p_o f_c f_e]\varepsilon_e + [p_o f_c f_h]\varepsilon_h = [p_o f_c f_o] \\
&[p_o f_d f_a]\varepsilon_a + [p_o f_d f_b]\varepsilon_b + [p_o f_d f_c]\varepsilon_c + [p_o f_d f_d]\varepsilon_d + [p_o f_d f_e]\varepsilon_e + [p_o f_d f_h]\varepsilon_h = [p_o f_d f_o] \\
&[p_o f_e f_a]\varepsilon_a + [p_o f_e f_b]\varepsilon_b + [p_o f_e f_c]\varepsilon_c + [p_o f_e f_d]\varepsilon_d + [p_o f_e f_e]\varepsilon_e + [p_o f_e f_h]\varepsilon_h = [p_o f_e f_o] \\
&[p_o f_h f_a]\varepsilon_a + [p_o f_h f_b]\varepsilon_b + [p_o f_h f_c]\varepsilon_c + [p_o f_h f_d]\varepsilon_d + [p_o f_h f_e]\varepsilon_e + [p_o f_e f_h]\varepsilon_h = [p_o f_e f_o].
\end{aligned} \tag{10}$$

Symbols that describe Eq.(10) are defined as

$$[p_o f_a f_b] = \sum_{i=1}^{n} p_{oi} f_{bi} f_{ai} = p_{o1} f_{b1} f_{a1} + p_{o2} f_{b2} f_{a2} + \cdots + p_{on} f_{bn} f_{an}$$

And so forth.

We can calculate $\varepsilon_a, \varepsilon_b, \ldots, \varepsilon_h$, by solving Eq.(10). Then substituting $\varepsilon_a, \varepsilon_b, \ldots, \varepsilon_h$, into Eq.(3), we can finally obtain $a,b,\ldots,h$.

For example in the case of ellipsoid, let calculate the concerning differential coefficients of the function f of the ellipsoid by using Eq.(1) as follows.

$$\frac{\partial f}{\partial x}=2(ax+by+cz)$$

$$\frac{\partial f}{\partial y}=2(bx+dy+ez)$$

$$\frac{\partial f}{\partial z}=2(cx+ey+hz)$$

$$\frac{\partial f}{\partial a} = x^2;\ \frac{\partial f}{\partial b} = 2xy;\ \frac{\partial f}{\partial c} = 2zx;\ \frac{\partial f}{\partial d} = y^2;\ \frac{\partial f}{\partial e} = 2yz;\ \frac{\partial f}{\partial h} = z^2.$$

Then Eq.(5) becomes

$$f_{oi} = a'X_i^2 + 2b'X_iY_i + 2c'Z_iX_i + d'Y_i^2 + 2e'Y_iZ_i + h'Z_i^2 - 1$$

$$f_{xi} = 2\left(a'X_i + b'Y_i + c'Z_i\right)$$

$$f_{yi} = 2\left(b'X_i + d'Y_i + e'Z_i\right)$$

$$f_{zi} = 2\left(c'X_i + e'Y_i + h'Z_i\right)$$

$$f_{ai} = X_i^2;\ f_{bi} = 2X_iY_i;\ f_{ci} = 2Z_iX_i;\ f_{di} = Y_i^2;\ f_{ei} = 2Y_iZ_i;\ f_{hi} = Z_i^2.$$

The expression of p_{oi} is

$$\frac{1}{p_{oi}} = \frac{f_{xi}f_{xi}}{p_{xi}} + \frac{f_{yi}f_{yi}}{p_{yi}} + \frac{f_{zi}f_{zi}}{p_{zi}}.$$

Supposing all the weights to be unity, that is, $p_{xi} = p_{yi} = p_{zi} = 1$, the simpler expression of p_{oi} becomes

$$p_{oi} = \frac{1}{f_{xi}^2 + f_{yi}^2 + f_{zi}^2}.$$

2.4 Procedure of three dimensional strain analysis by means of the least square strain technique

(1) Cut out three non-parallel planes from oriented rock samples and name them as planes A, B and C.

(2) Calculate the direction of long axis and the axial ratio of the strain ellipses on the planes A, B and C by means of the two dimensional strain analysis.

(3) Calculate the relative axial length of the strain ellipses by the GS method.

(4) Calculate the shape tensor of the strain ellipsoid that is constructed from the strain ellipses by the least square strain technique.

(5) Calculate the axial lengths X, Y and Z using the eigen values of the shape tensor C of the strain ellipsoid. Supposing that λ_1, λ_2 and λ_3 are the eigen values of C and that

$$\lambda_1 < \lambda_2 < \lambda_3$$

,we have the axial lengths of the strain ellipsoid as

$$X = \sqrt{\frac{1}{\lambda_1}}, \quad Y = \sqrt{\frac{1}{\lambda_2}}, \quad Z = \sqrt{\frac{1}{\lambda_3}}$$

,where X>Y>Z.

(6) Calculate the direction of X, Y and Z of the strain ellipsoid using the eigen vectors of C. The direction of X, Y and Z equals that of the eigen vectors that correspond with λ_1, λ_2 and λ_3, respectively.

3. Precision of three dimensional strain analysis performed by the least square strain technique

3.1 Property of strain marker

Strain marker is assumed to have the following properties.

(1) Shape of the marker is ellipsoid.
(2) There is no competency contrast between the marker and the matrix.
(3) Direction of the initial principal axes of the marker is random.
(4) Markers are homogeneously deformed.
(5) Markers do not change their volume during deformation (refer to Appendix A).
(6) The axial ratio ($R_i = \frac{X_i}{Z_i}$) of the markers shows normal distribution.

The assumptions from (1) to (4) are the same those in the case of two dimensional finite strain analysis using ellipse-shape strain markers. I have supposed that the conditions of (5) and (6) are reasonable for the natural strain markers.

3.2 Models

I have examined how the following three factors affect to the precision of the least square strain technique, assuming that the axial ratio of the strain markers shows normal distribution.

(1) Variation of the sample size of the strain markers
(2) Variation of the mean of the axial ratio of the strain markers
(3) Variation of the standard deviation of the axial ratio of the strain markers

Three series including twelve models are produced to perform the aim. Ten models within the twelve's are independent because the model 38 is used repeatedly third times in the different series.

(1) Series A

The sample size (n) of the markers varies, though the mean (m) of the axial ratio of the markers is fixed as 2 and the standard deviation (σ) of the axial ratio of the markers is fixed as $\frac{1}{6}$ The series is composed of the following four models.

model 44 $n = 100$
model 38 $n = 300$

model 45 n = 600
model 46 n = 1000

(2) Series B

The mean (m) of the axial ratio of the markers varies, though the sample size(n) and the standard deviation (σ) are fixed as n=300 and $\sigma = \frac{1}{6}$. The series includes the following three models.

model 38 m = 2
model 39 m = 3
model 40 m = 4

(3) Series C

The standard deviation (σ)of the axial ratio of the markers varies, though the sample size (n) and the mean (m) of the axial ratio of the markers are fixed as n=300 and m=2. The series includes the following five models.

model 38 $\sigma = \frac{1}{6}$.

model 50 $\sigma = \frac{1}{8}$.

model 51 $\sigma = \frac{1}{10}$.

model 52 $\sigma = \frac{1}{12}$.

model 41 σ = 0.

3.3 Preparing marker ellipsoids

3.3.1 Producing normal random numbers whose mean is m and standard deviation is σ

Normal random number is produced from uniform random number by the Box and Müller method. Using two uniform random numbers u_i and u_{i+1} , the normal random numbers z_i and z_{i+1} whose mean and standard deviation are m and σ, are calculated by the equations.

$$z_i = \sqrt{-2\log u_i}(\cos 2\pi)(u_{i+1})\sigma + m$$

$$z_{i+1} = \sqrt{-2\log u_i}(\sin 2\pi)(u_{i+1}) + m$$

The axial ratio (R_i)of marker ellipsoids is assumed to the normal random number.

3.3.2 Producing two axial lengths of marker ellipsoid whose axial ratio is R_i

Being different to the case of a point of strain ellipsoid (strain point), a point of marker ellipsoid (marker point) does not lie on the curve X_i Z_i=1 on X_i Z_i diagram (refer to Appendix A). Thus we cannot locate the marker point by R_i, but we should represent the marker point on the X_i Z_i diagram by the two axial lengths, X_i and Z_i . We pay attention that Y_i is defined as unity. On the X_i Z_i diagram (Fig.3), the

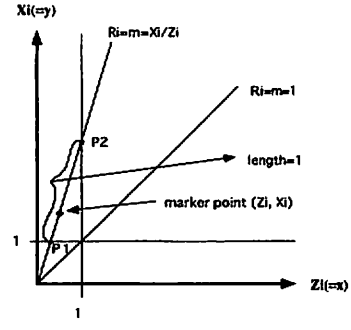

Fig.3 X_i Z_i diagram. Y_i is defined to be unity. P_1 is the intersecting point of a line y=mx and a line y=1. P_2 is the intersecting point of y=mx and x=1. The distance between P_1 and P_2 is unity.

intersecting point of a line $X_i=R_i Z_i$ and a line $X_i=1$ is P_1 and the intersecting point of a line $X_i=R_i Z_i$ and $Z_i=1$ is P_2. The distance between P_1 and P_2 is assumed to be unity. We define arbitrarily a marker point (Z_i, X_i) by producing a random number among 0 to 1 as follows. On the $X_i Z_i$ diagram, let rewrite the variable Z_i to x as abscissa and variable X_i to y as ordinate, and R_i to m. Since the point P_1 is the intersection of both the lines

$$\begin{cases} y = mx \\ y = 1 \end{cases}$$

, we have the coordinate of P_1 as $\left(\frac{1}{m},\ 1\right)$. Similarly for the point P_2 which is the intersection of

$$\begin{cases} y = mx \\ x = 1 \end{cases}$$

, we have P_2 as $(1, m)$. Therefore, when we divide equally the distance between P_1 and P_2 into n parts, the both increments of x and y are

$$\begin{cases} x_{inc} = \dfrac{\left(1-\frac{1}{m}\right)}{n} \\ y_{inc} = \dfrac{(m-1)}{n} \end{cases}.$$

We have the coordinate (x_k, y_k) of the k th point as

$$\begin{cases} x_k = \dfrac{1}{m} + \left(1-\dfrac{1}{m}\right)\dfrac{k}{n} \\ y_k = 1 + (m-1)\dfrac{k}{n} \end{cases}.$$

If we want to produce random points ranging between P_1 and P_2 on the line $y=mx$, we exchange a value of $\frac{k}{n}$ to a random number among 0 to 1. If we have calculated the coordinate (x_k, y_k) in this manner, the (x_k, y_k) could be the coordinate of a random marker point (Z_i, X_i). Since $Y_i=1$ on the $X_i Z_i$ diagram, three axial lengths of the marker ellipsoid are obtained as X_i, 1 and Z_i .Thus the distribution of initial marker points regarding a couple of typical model is illustrated in Fig.4.

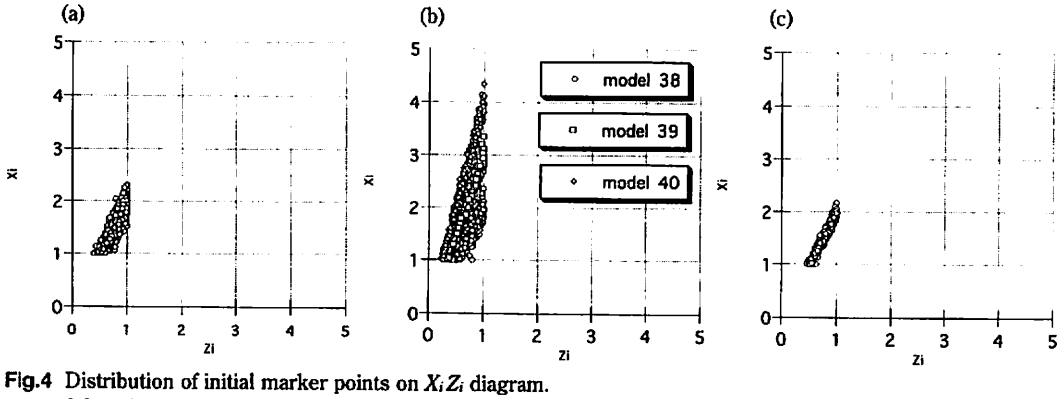

Fig.4 Distribution of initial marker points on $X_i Z_i$ diagram.
a : model 46 (sample size is 1000) as an example of the series A. b : models 38,39 and 40 (m is 2, 3 and 4) of the series B. c : model 52 (σ is $\frac{1}{12}$) as an example of the series C.

3.3.3 Random distribution of principal axes of marker ellipsoid

Producing the marker ellipsoid whose axes are randomly oriented has the same meaning that we produce an orthogonal XYZ system that rotates arbitrarily around an orthogonal xyz coordinate system. If the direction of the X axis is indicated by the Euler angle (α, β, γ), we have

$$\cos^2\alpha + \cos^2\beta + \cos^2\gamma = 1$$

The formula is changed into

$$\cos\gamma = \pm\sqrt{1-\cos^2\alpha-\cos^2\beta}.$$

The X, Y and Z axes are calculated by the following procedure.

(1) Define α and β randomly.

(2) Define γ using the above formula. Then X axis is obtained.

(3) Repeat the calculation from (1) to (2), and define the other axis which is called P axis.

(4) Define Y axis as the intersection of two planes whose poles are X and P axes.

(5) Define Z axis as the vector product of X and Y axes.

3.3.4 Representation of marker ellipsoid in xyz system

Taking the orthogonal XYZ system that is produced at the section 3.3.3 to the present coordinate system, we write marker ellipsoid as follows.

$\mathbf{X}^T A\mathbf{X} = 1$

The equation of the ellipsoid can be changed to the equation that is presented in the other coordinate xyz system if we know the transform tensor between the two coordinate systems. The transform tensor is supposed here as

$$\mathbf{X} = T\mathbf{x}$$

where

$$T = \begin{bmatrix} \cos\theta_{11} & \cos\theta_{12} & \cos\theta_{13} \\ \cos\theta_{21} & \cos\theta_{22} & \cos\theta_{23} \\ \cos\theta_{31} & \cos\theta_{32} & \cos\theta_{33} \end{bmatrix}.$$

The Euler angle of X axis is ($\cos\theta_{11}$, $\cos\theta_{12}$, $\cos\theta_{13}$) and those of Y and Z axes are ($\cos\theta_{21}$, $\cos\theta_{22}$, $\cos\theta_{23}$) and ($\cos\theta_{31}$, $\cos\theta_{32}$, $\cos\theta_{33}$), respectively as illustrated in Fig.5. The marker ellipsoid described in the xyz system is

$$(T\mathbf{x})^T A(T\mathbf{x}) = 1$$
$$\mathbf{x}^T(T^T AT)\mathbf{x} = 1.$$

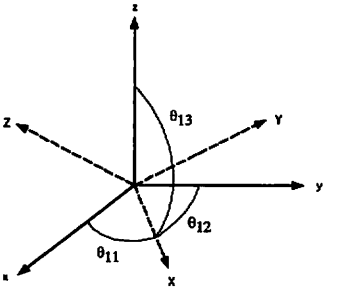

Fig.5 Two orthogonal coordinate systems, xyz and XYZ.

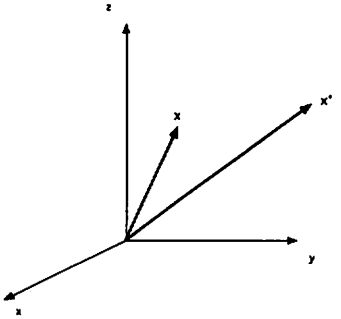

Fig.6 A place vector x presented in xyz coordinate system. The vector x is transformed into vector x' by deformation tensor G.

3.4 Deformation of marker ellipsoid

Showing in Fig.6, let transform a place vector x into x' by the deformation tensor G (refer to Appendix D).

$$\mathbf{x}' = G\mathbf{x}$$

We rewrite it to

$\mathbf{x} = G^{-1}\mathbf{x}'$.

Supposing the marker ellipsoid before deformation as

$\mathbf{x}^T A\mathbf{x} = 1$

, the marker ellipsoid after deformation becomes

$\mathbf{x}'^T(G^{-1})^T AG^{-1}\mathbf{x}' = 1$.

For each model the marker ellipsoid is deformed ninety times varying the axial ratio (R) of strain ellipsoid from 1.1 to 10 at interval 0.1.

3.5 Precision of models of each series

Regarding three series including twelve models described in the section 3.2, strain ellipsoid is calculated by the least square strain method. We cannot clearly recognize the difference between the calculated strain and the true strain on the normalized Flinn diagram** since the difference is small. Thus I take the distance between the calculated and the true strain points on the normalized Flinn diagram as a parameter of strain precision, which is called "distance precision".

3.5.1 Distance precision of models of each series

In order to compare the models of each series, I have used the diagram where the distance precision is taken as ordinate and the axial ratio (R) of true strain is taken as abscissa. It seems that the strain precision does not depend on the sample size from Fig.7a*** for the series A. When the value of strain is larger, the order of the distance precision of each sample size changes. Thus the sample size does not clearly depend on the strain precision. From Fig.7b for the series B, when the mean of the axial ratio of marker ellipsoids is small, the strain precision is high. From Fig.7c for the series C, the standard deviation of the axial ratio of the marker ellipsoids does not

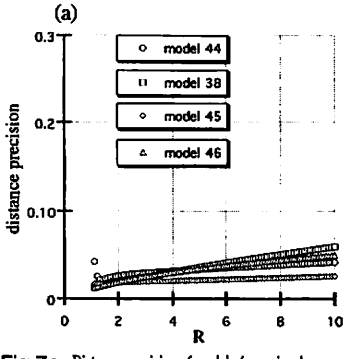

Fig.7a Distance precision of models for series A. Distance precision is taken as ordinate. Abscissa shows true strain ratio R. The distance precision is the distance between the calculated and the true strain points on the normalized Flinn diagram.

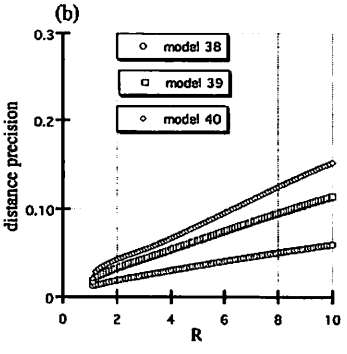

Fig.7b Distance precision of models for series B. Others are same as in Fig.7a.

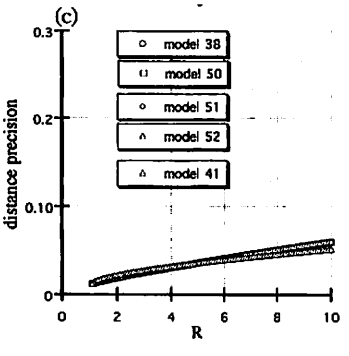

Fig.7c Distance precision of models for series C. Others are same as in Fig.7a.

** The normalized Flinn diagram is the Flinn diagram where the length of Y axis is defined unity. As a result the abscissa is 1/Z and the ordinate is X in this diagram.

*** One or two points near R=1 on Fig.7a is deviated from the curve. This might be due to the instability of the calculation.

relate to the strain precision.

3.5.2 Angle precision of models of each series

In order to compare the angular precision of the models of each series, I have used the diagram whose ordinate is angle precision and abscissa is R. The angle precision is the difference between the direction of the long (X) axis of the calculated and the true strain ellipsoid. Since the tendency of three principal axes X, Y and Z are almost the same, the tendency with regard to the X axis is described as the representative of the three axes.

Fig.8a for series A shows that the angle precision of X axis is low in the model of 100 sample size than that of other sample sizes, and among the other sample sizes the angle precision of them is almost same. Fig.8b for series B indicates that when the mean of the axial ratio of marker ellipsoids is small, the angle precision of X axis becomes high. Fig.8c for series C shows that the angle precision of X axis is independent of the standard deviation of the axial ratio of marker ellipsoids.

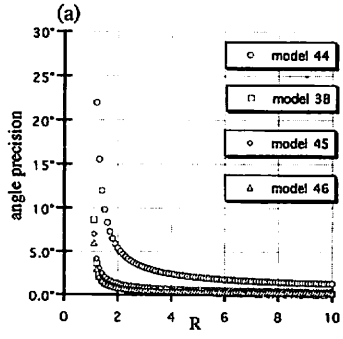

Fig.8a Angle precision of models for series A. Angle precision is taken as ordinate. Abscissa indicates true strain ratio R. The angle precision is the difference of angle between the X axis of the calculated and the true strain ellipsoid.

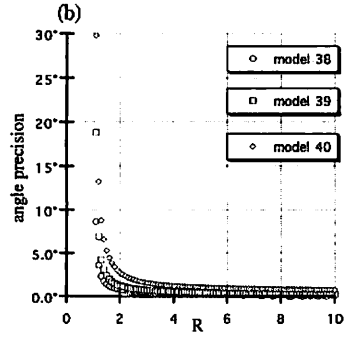

Fig.8b Angle precision of models for series B. Others are same as in Fig.8a.

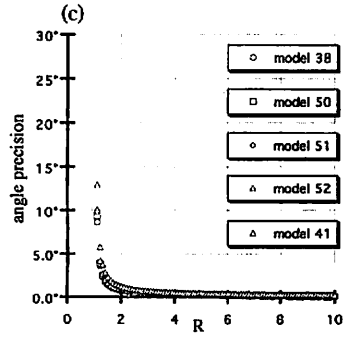

Fig.8c Angle precision of models for series C. Others are same as in Fig.8a.

Three items are concluded from the description of the sections 3.5.1 and 3.5.2 that (1) the relation between the strain precision and the sample size of marker ellipsoids is unclear, (2) the strain precision is high, when the mean of the axial ratio of marker ellipsoids takes a small value, (3) the strain precision is independent of the standard deviation of the axial ratio of marker ellipsoids.

3.6 Method to estimate the normalized distance of surface point

The normalized distance is the concept of another precision of strain described by the calculated and the true strain ellipsoids themselves. The method was originally developed by Hayashi(1995). The method is described briefly as follows. As shown in Fig.1 , let cut a strain ellipsoid through non-parallel planes A, B and C. If we divide one twelfth every 30° the arc of a strain ellipse as illustrated in Fig.9 where the strain ellipse is a section of the strain ellipsoid, we have located 36 points on the three planes. I call the 36 points "surface points" since they lie on the surface of the strain ellipsoid. In Fig.10, we represent any vector **p** as

$$\mathbf{p} = \begin{pmatrix} x \\ y \\ z \end{pmatrix}.$$

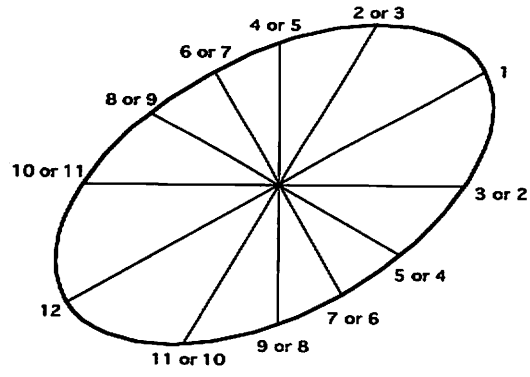

Fig.9 Twelve surface points on a strain ellipse. They divide the ellipse at interval of 30°.

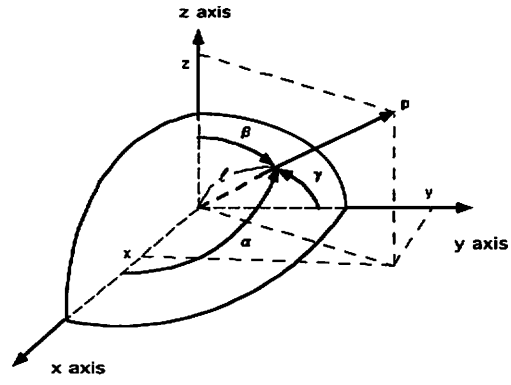

Fig.10 A direction vector $\boldsymbol{p}$ is denoted by Euler angle (α,β,γ) and its coordinate is (x,y,z). An intersecting point between $\boldsymbol{p}$ and the surface of the ellipsoid shows distance l from the origin.

We have the next relation with regard to any vector **p**

$$|\mathbf{p}| = \sqrt{x^2 + y^2 + z^2}$$

where

$$\cos\alpha = \frac{x}{|\mathbf{p}|},\ \cos\beta = \frac{y}{|\mathbf{p}|},\ \cos\gamma = \frac{z}{|\mathbf{p}|}.$$

Suppose that $\boldsymbol{p}$ lies on the ellipsoid

$$(x\ \ y\ \ z)\begin{bmatrix} a & b & c \\ & d & e \\ sym & & h \end{bmatrix}\begin{pmatrix} x \\ y \\ z \end{pmatrix} = 1. \qquad (11)$$

Eq.(11) is rewritten as

$$ax^2 + 2bxy + 2czx + dy^2 + 2eyz + hz^2 = 1.$$

Suppose the distance between the surface point and the center of the ellipsoid to be l. The surface point is the point that intersects the vector **p** and the surface of the ellipsoid. We have relations

$$x = l\cos\alpha,\ y = l\cos\beta,\ z = l\cos\gamma$$

and

$$l^2(a\cos^2\alpha + 2b\cos\alpha\cos\beta + 2c\cos\gamma\cos\alpha + d\cos^2\beta + 2e\cos\beta\cos\gamma + h\cos^2\gamma) = 1. \qquad (12)$$

I have calculated by using Eq.(12) the distance (E_t) of a point (P_t) that lies on the surface of the true strain ellipsoid measured from its center. I have also calculated the distance (E_c) of a point (P_c) that lies on the surface of the calculated strain ellipsoid measured from its center. If the direction of both the points P_t and P_c is same, the difference between E_c and E_t are denoted E_{ct} ($=E_c - E_t$). When E_{ct} is divided by E_t, I call it N_{ct}. N_{ct} is the value that is the normalized distance between a surface point of the true strain ellipsoid and that of the calculated strain ellipsoid, and I call N_{ct} "normalized distance of surface point".

Fig.11 shows the normalized distance of the 36 surface points at R=1.1 for the model 38. In Fig.11 the surface point number is taken as abscissa and the normalized distance (N_{ct}) as ordinate. In the figure, the line N_{ct}=0 indicates the surface of the true strain ellipsoid. The open circles represent the normalized distance (N_{ct}) of the 36 surface points. When the open circle approaches toward

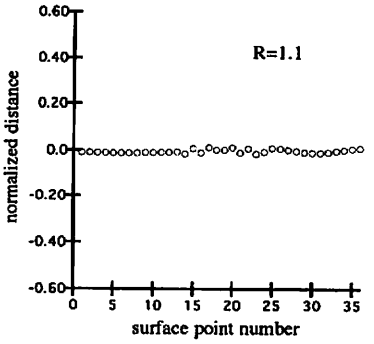

Fig.11 Normalized distance (*Nct*) of 36 surface points at R=1.1 for the model 38. *Nct* = 0 means the surface of true strain ellipsoid.

the line N_{ct}=0, the calculated strain closes to the true strain.

3.7 Comparison of strain precision of models by deviation range

Markers of each model have received 90 stages of deformation recorded by the strain axial ratio (R). R changes from 1.1 to 10 at interval 0.1. The mean and the standard deviation of the normalized distance of the 36 surface points in every stage of deformation are calculated. In Fig.12 the deviation range of all the models is plotted with the strain axial ratio (R) as abscissa and the normalized distance (N_{ct}) as ordinate. In the figure the deviation range of the 36 surface points for each R is drawn by the parallel line to the ordinate axis. The center of the parallel line indicates the mean of N_{ct} of the 36 surface points. The length of the line equals to two times of the standard deviation of N_{ct} of the 36 surface points.

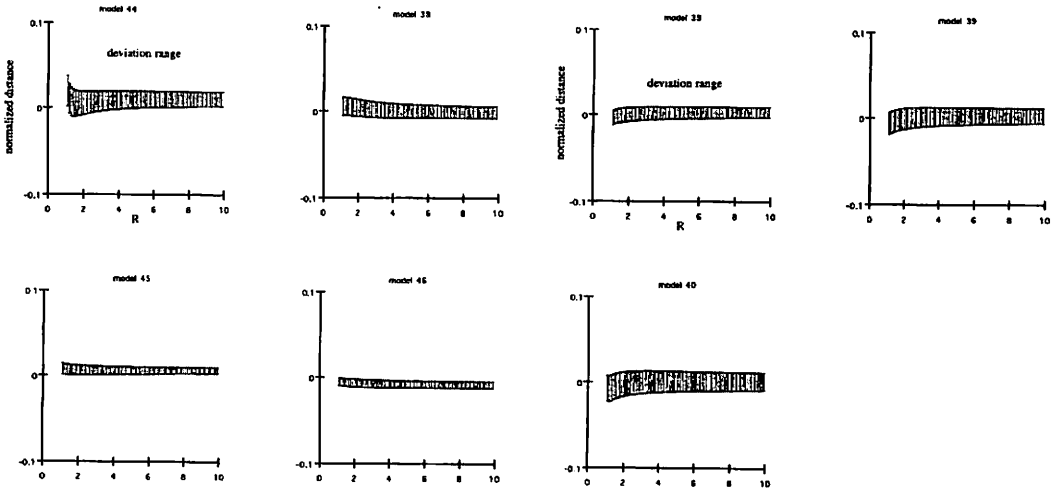

Fig.12a Deviation range for series of A.
Deviation range of 36 surface points indicated for 90 stages of strain axial ratio R (abscissa). Ordinate is taken by the normalized distance. R varies from 1.1 to 10.

Fig.12b Deviation range for series of B. Others are same as in Fig.12a.

Regarding the series A, from Fig.12a we can see that when the sample size of marker ellipsoids increases from 100 to 1000, the deviation range of the 36 surface points becomes narrow. The strain precision becomes higher in this order. For the series B, from Fig.12b we know that when the mean of the axial ratio (R_i) of initial marker ellipsoids increases from 2 to 4, the deviation range of the 36 surface points grows wider. The strain precision becomes lower in this order. As regard to the series C, from Fig.12c we agree that when the standard deviation of the axial ratio (R_i) of initial marker ellipsoids decreases from $\frac{1}{6}$ to 0, the deviation range of the 36

surface points does not vary. The strain precision does not change.

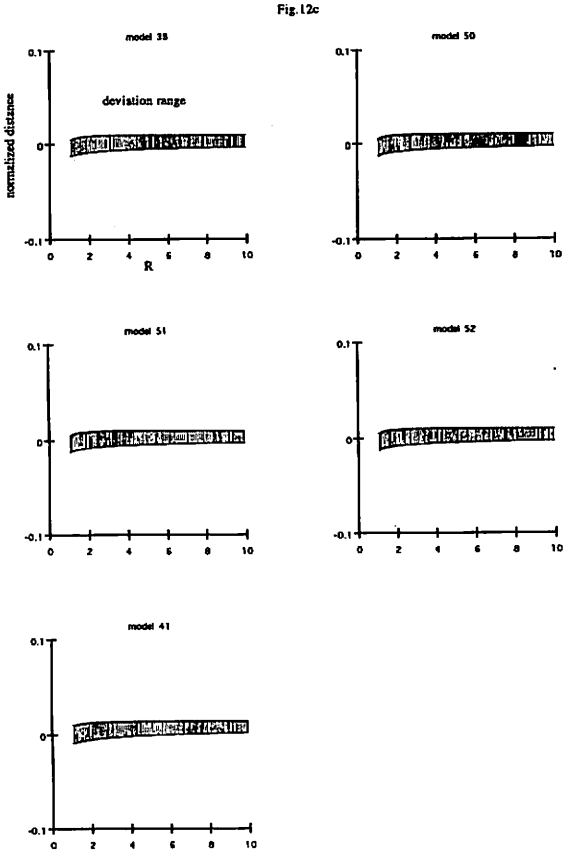

Fig.12c Deviation range for series of C. Others are same as in Fig.12a.

4. Discussion

4.1 Randomness test of the normal random number

The present simulation assumes that the axial ratio (R_i) of initial marker ellipsoids shows normal distribution. We should examine how the distribution of the normal random number fit to normal distribution.

I have used the χ^2 test (test of goodness of fitness) for the examination. The χ^2 test is the test whether an empirical distribution (sample distribution) fit well to a theoretical distribution (distribution of population).

Considering an empirical and a theoretical distribution as $\{f_i\}$ and $\{f_i^*\}$ (i=1 to k), the formula of χ^2 is defined as follows.

$$\chi^2 = \sum_{i=1}^{k} \frac{(f_i - f_i^*)^2}{f_i^*}$$

When we compare the values of χ^2 and χ^2_α, and if we have

$\chi^2 > \chi^2_\alpha$

, then we should abandon the hypothesis at α. The hypothesis is "sample is a random sample of population". χ^2_α is the χ^2 value at the level of significance and at the freedom

$\varphi = k - 1$****.

In the present paper there are four sample sizes, n=100, 300, 600 and 1000. We designate the normal distribution of $m = 0$ and $\sigma = 1$ as "$N(0, 1^2)$". Since the shape of any normal distribution is independent on its mean and standard deviation but depends on its sample size, we should examine the $N(0, 1^2)$ of four sample sizes instead of all the normal distributions of various means and of various standard deviations.

The equation of the $N(0, 1^2)$ is represented as

$$\varphi = \frac{1}{\sqrt{2\pi}}\exp\left(-\frac{z^2}{2}\right)$$

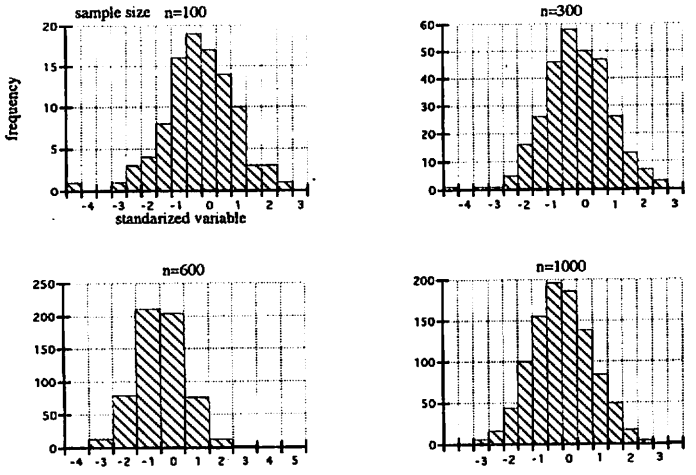

Fig.13 Distribution of R_i indicated by frequency histogram for normal random number. Sample sizes are 100, 300, 600 and 1000.

level of significance α	value of χ^2_α
0.99	1.24
0.95	2.17
0.90	2.83
0.75	4.25
0.50	6.35
0.25	9.04
0.1	12.02
0.05	14.07
0.01	18.48
0.005	20.3

Table 1 Value of χ^2_α . χ^2_α is the value of χ^2 where the level of significance α changes from 0.99 to 0.005 and the freedom is 7.

where z is the standardized variable. The probability of the normal distribution within the range $[z_1, z_2]$ is calculated by

$$\int_{z_1}^{z_2} \varphi(z)dz$$

which is equal to the frequency of the theoretical distribution. I have calculated four χ^2 values for four sample sizes as follows.

$\chi^2 = 1.82$ at $n = 100$

$\chi^2 = 2.77$ at $n = 300$

$\chi^2 = 2.38$ at $n = 600$

$\chi^2 = 3.41$ at $n = 1000$

The distribution of R_i denoted by histogram is shown in Fig.13 at each sample size 100, 300, 600 and 1000. The value of χ^2_α is shown on Table 1. χ^2_α is the value of χ^2 at the level of significance

**** When we consider a theoretical distribution as a normal distribution, we do not take the freedom as $\varphi = k - 1$ but as $\varphi = k - 3$.

(α) where α varies from 0.99 to 0.005 and the freedom is 7. From the table we know that all the χ^2 values calculated for four sample sizes are small enough compared to the χ^2_α value. The normal random number thus produced is well coincide with normal distribution.

4.2 Randomness test of the uniform random number

We need uniform random number to define three axial lengths of a marker ellipsoid whose axial ratio is given. The uniform random number is also examined by the χ^2 test.
The χ^2 values for four sample sizes are calculated as follows.
$\chi^2 = 3.6$ at $n = 100$
$\chi^2 = 3.4$ at $n = 300$
$\chi^2 = 3$ at $n = 600$
$\chi^2 = 5$ at $n = 1000$
The distribution of R_i is shown in Fig.14. The χ^2_α values where the level of significance α varies from 0.99 to 0.005 and the freedom is 9, are indicated on Table 2. From the table we agree that the χ^2 values calculated for four sample sizes are small enough compared to the χ^2_α values. The uniform random numbers thus produced are well random to use for the present simulation.

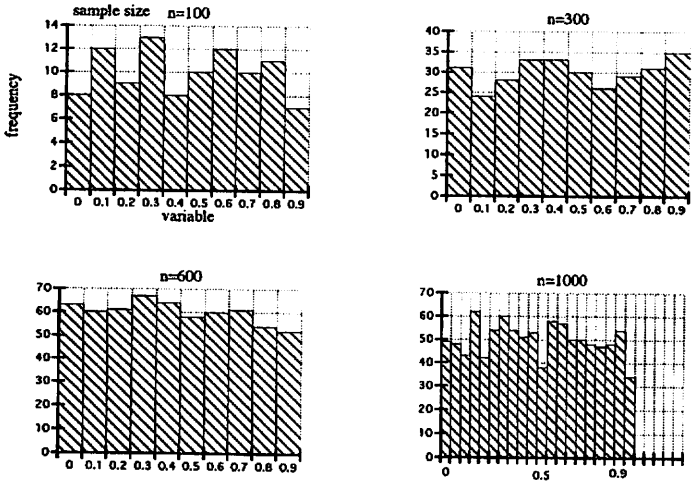

Fig.14 Distribution of R_i indicated by frequency histogram for uniform random number. Sample sizes are 100, 300, 600 and 1000.

level of significance α	value of χ^2_α
0.99	2.09
0.95	3.33
0.90	4.17
0.75	5.90
0.50	8.34
0.25	11.39
0.1	14.68
0.05	16.92
0.01	21.7
0.05	23.6

Table 2 Value of χ^2_α where α varies from 0.99 to 0.005 and the freedom is 9.

4.3 Randomness test of the principal direction of initial marker ellipsoids (by Woodcock and Naylor's randomness test)

We should examine whether the principal direction of initial marker ellipsoids is random or not. I have examined the randomness by the method developed by Woodcock and Naylor (1983). The randomness test needs not to perform for all the models but for four sample sizes, 100, 300, 600 and 1000. The $\frac{S_1}{S_3}$ values for X, Y and Z axes in each case are shown on Table 3a. The critical

sample size (n)	$\frac{S_1}{S_3}$ value of X axis	$\frac{S_1}{S_3}$ value of Y axis	$\frac{S_1}{S_3}$ value of Z axis
100	1.34601	1.23464	1.31795
300	1.16250	1.11528	1.20014
600	1.10568	1.04090	1.07448
1000	1.08414	1.07467	1.05081

Table 3a

values of $\frac{S_1}{S_3}$ that were calculated by Woodcock and Naylor (1983) are also shown on Table 3b. Comparing both tables we can say that the principal direction of the initial marker ellipsoids is random for every sample size.

sample size (n)	confidence level 90%	confidence level 95%	confidence level 97.5%	confidence level 99%
100	1.597	1.667	1.736	1.82
300	1.30	1.34	1.38	1.44
600	1.20	1.23	1.26	1.29
1000	1.161	1.177	1.192	1.207

Table 3b

Table 3 Woodcock and Naylor's randomness test.

a : $\frac{S_1}{S_3}$ value of X, Y and Z axes for each sample size 100, 300, 600 and 1000.

b : Critical value of $\frac{S_1}{S_3}$ for each sample size 100, 300, 600 and 1000 (Woodcock and Naylor,1983).

4.4 Randomness test of the principal direction of initial marker ellipsoids (by the calculation of strain ellipse)

If the principal direction of initial marker ellipsoids distributes randomly, and assuming the axial ratio (R_i) and the direction (θ) of long axis of initial marker ellipses as R_f and ϕ of the deformed marker ellipses, the strain ellipse becomes a circle. The axial ratio (R) of the strain ellipse with respect to non-deformation is unity. The axial ratio of all the strain ellipses during non-deformation in every model is indicated on Table 4. From the table we know that the principal direction of the initial marker ellipsoids in every model is random.

model	axial ratio (R) on xy-plane	axial ratio (R) on yz-plane	axial ratio (R) on xz-plane
model 38	1.013	1.023	1.023
model 39	1.022	1.034	1.033
model 40	1.029	1.040	1.039
model 41	1.020	1.029	1.019
model 44	1.079	1.034	1.015
model 45	1.020	1.009	1.011
model 46	1.014	1.004	1.012
model 50	1.013	1.024	1.023
model 51	1.014	1.024	1.023
model 52	1.014	1.024	1.023

Table 4 Axial ratio of strain ellipse for non-deformation in each model.

Appendix A *XZ diagram representation of the strain point referred by the axial ratio (R) of strain ellipsoid*

Define the axial ratio (R) of a strain ellipsoid as $R = \frac{X}{Z}$, then R means the gradient of a line through the origin (0,0) as illustrated in Fig.15. I call the figure "XZ diagram". Assuming that the volume of marker ellipsoids does not change before and after deformation, the strain point (Z, X) lies on a curve XZ=1. Thus we need to solve the next simultaneous equations to obtain the values of X and Z with regard to the axial ratio (R).

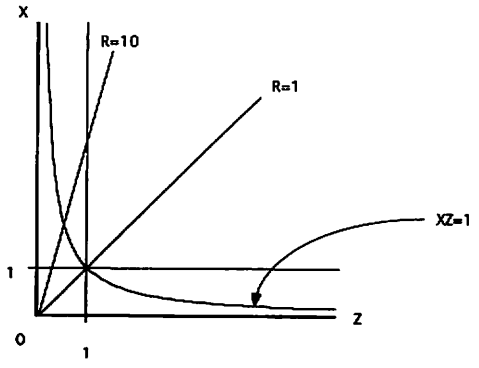

Fig.15 XZ diagram where X and Z mean the long and the short axial length of strain ellipsoid. X and Z show ordinate and abscissa, respectively.

$$\begin{cases} X = RZ \\ XZ = 1 \end{cases}$$

We have the strain point (Z,X) regarding

the axial ratio (R) as $\left(\frac{1}{\sqrt{R}},\ \sqrt{R}\right)$.

Appendix B *Representation of the shape tensor of strain ellipsoid by means of the axial ratio (R)*

Using the axial ratio (R) we can write the normalized axial lengths as $\left(X=\sqrt{R},\ Y=1,\ Z=\frac{1}{\sqrt{R}}\right)$ by referring Appendix A. The equation of strain ellipsoid where X, Y and Z axes are coincide with x, y and z axes, is written as

$$\mathbf{x}^T F^{-1} \mathbf{x} = 1 \tag{B1}$$

where F is the finger tensor. The inverse tensor of F is the shape tensor of the ellipsoid. If we write F^{-1} as

$$\begin{bmatrix} a & 0 & 0 \\ & b & 0 \\ sym & & c \end{bmatrix}$$

, Eq.(B1) is

$$\mathbf{x}^T \begin{bmatrix} a & 0 & 0 \\ & b & 0 \\ sym & & c \end{bmatrix} \mathbf{x} = 1. \tag{B2}$$

Eq.(B2) is expanded to

$$ax^2 + by^2 + cz^2 = 1. \tag{B3}$$

Eq.(B3) is changed to

$$\frac{x^2}{\left(\frac{1}{\sqrt{a}}\right)^2} + \frac{y^2}{\left(\frac{1}{\sqrt{b}}\right)^2} + \frac{z^2}{\left(\frac{1}{\sqrt{c}}\right)^2} = 1. \tag{B4}$$

Considering that Eq.(B4) is the equation of strain ellipsoid, the following equations hold.

$$\begin{cases} X = \frac{1}{\sqrt{a}} \\ Y = \frac{1}{\sqrt{b}} = 1 \\ Z = \frac{1}{\sqrt{c}} \end{cases} \tag{B5}$$

We have next relations from Eq.(B5).

$$a = \frac{1}{X^2},\ b = 1,\ c = \frac{1}{Z^2}$$

Finally we have the shape tensor of the strain ellipsoid as follows.

$$F^{-1} = \begin{bmatrix} \frac{1}{X^2} & 0 & 0 \\ & 1 & 0 \\ sym & & \frac{1}{Z^2} \end{bmatrix} = \begin{bmatrix} \frac{1}{R} & 0 & 0 \\ & 1 & 0 \\ sym & & R \end{bmatrix}$$

Appendix C *Representation of the deformation tensor by means of the axial ratio (R) of strain ellipsoid (1)*

When the principal axes X, Y and Z of strain ellipsoid coincide with the coordinate axes x, y and z, how we represent the deformation tensor by the axial ratio (R) of the strain ellipsoid. Since we have the shape tensor F^{-1} of the strain ellipsoid written by the axial ratio (R) as described in Appendix B, the finger tensor F of the strain ellipsoid is given as follows.

$$F = \begin{bmatrix} X^2 & 0 & 0 \\ & 1 & 0 \\ sym & & Z^2 \end{bmatrix} \tag{C1}$$

The definition of the finger tensor is

$$F = DD^T \tag{C2}$$

where D is the deformation tensor indicated as follows.

$$D = \begin{bmatrix} a & 0 & 0 \\ & b & 0 \\ sym & & c \end{bmatrix} \tag{C3}$$

From Eqs.(C2) and (C3) we have

$$F = \begin{bmatrix} a & 0 & 0 \\ & b & 0 \\ sym & & c \end{bmatrix}\begin{bmatrix} a & 0 & 0 \\ & b & 0 \\ sym & & c \end{bmatrix} = \begin{bmatrix} a^2 & 0 & 0 \\ & b^2 & 0 \\ sym & & c^2 \end{bmatrix}. \tag{C4}$$

As Eq.(C4) equals to Eq.(C1) ,we have the deformation tensor presented by R as follows.

$$D = \begin{bmatrix} X & 0 & 0 \\ & 1 & 0 \\ sym & & Z \end{bmatrix} = \begin{bmatrix} \sqrt{R} & 0 & 0 \\ & 1 & 0 \\ sym & & \frac{1}{\sqrt{R}} \end{bmatrix}$$

Appendix D *Representation of the deformation tensor by means of the axial ratio (R) of strain ellipsoid (2)*

When the principal axes X, Y and Z of a strain ellipsoid do not coincide with the coordinate axes x, y and z, how we obtain the deformation tensor presented by the axial ratio (R) of the strain

ellipsoid and the coordinate transform tensor T. As shown in Fig.5 we choose the Euler angle of X, Y and Z axes in the xyz system as follows.

$(\cos\theta_{11}, \cos\theta_{12}, \cos\theta_{13})$ for X axis

$(\cos\theta_{21}, \cos\theta_{22}, \cos\theta_{23})$ for Y axis

$(\cos\theta_{31}, \cos\theta_{32}, \cos\theta_{33})$ for Z axis

Consider that **X** and **x** are the basis vectors and T is the transform tensor between them, then we have the next relation.

$$\mathbf{X} = T\mathbf{x} \qquad \text{(D1)}$$

where T is represented by the Euler angle as follows.

$$T = \begin{bmatrix} \cos\theta_{11} & \cos\theta_{12} & \cos\theta_{13} \\ \cos\theta_{21} & \cos\theta_{22} & \cos\theta_{23} \\ \cos\theta_{31} & \cos\theta_{32} & \cos\theta_{33} \end{bmatrix}$$

Assuming D as a deformation tensor and **X** is deformed by D to **x'**, we have

$$\mathbf{x}' = D\mathbf{X}.$$

This is inverted to

$$\mathbf{X} = D^{-1}\mathbf{x}'. \qquad \text{(D2)}$$

The equation of sphere that is represented in the XYZ coordinate system is

$$\mathbf{X}^T\mathbf{X} = 1. \qquad \text{(D3)}$$

Substituting Eq.(D2) into Eq.(D3), we have

$$(D^{-1}\mathbf{x}')^T(D^{-1}\mathbf{x}') = 1.$$

This is changed to

$$(\mathbf{x}')^T F^{-1}\mathbf{x}' = 1.$$

We replace **x'** with **X**, because D is not a transform tensor connecting two basis vectors and **x'** is a mere place vector. We have the equation of strain ellipsoid as

$$\mathbf{X}^T F^{-1}\mathbf{X} = 1. \qquad \text{(D4)}$$

When we transform Eq.(D4) by Eq.(D1), we have the equation of the strain ellipsoid that is described in the xyz coordinate system as follows.

$$\mathbf{x}^T(D^{-1}T)^T(D^{-1}T)\mathbf{x} = 1. \qquad \text{(D5)}$$

On the other hand the equation of sphere presented in the xyz system is

$$\mathbf{x}^T\mathbf{x} = 1. \qquad \text{(D6)}$$

Assuming the deformation tensor in the xyz system as G, we have

$$\mathbf{x}' = G\mathbf{x}$$

which is also written as

$$\mathbf{x} = G^{-1}\mathbf{x}'. \qquad \text{(D7)}$$

Substituting Eq.(D7) into Eq.(D6) and changing $\mathbf{x}'$ to $\mathbf{x}$, we have

$$\mathbf{x}^T(G^{-1})^T(G^{-1})\mathbf{x} = 1. \qquad \text{(D8)}$$

This is the equation of the strain ellipsoid presented in the xyz coordinate system. Comparing the equation (D8) to (D5), we have

$$G^{-1} = D^{-1}T$$

which is also written as

$$G = (D^{-1}T)^{-1} = T^{-1}D$$

As this is the deformation tensor presented in the xyz system, we can deform any marker ellipsoids by the deformation tensor G.

References

De Paor,D.G.,1990.Determination of the strain ellipsoid from sectional data.*J.Struct.Geol.*,12:131-137.

Dunnet,D.,1969.A technique of finite strain analysis using elliptical particles.*Tectonophysics*,7:117-136.

Elliott,D.,1970.Determination of finite strain and initial shape from deformed elliptical objects.*Geol.Soc.Am.Bull.*,81:2221-2236.

Fry,N.,1979.Random point distributions and strain measurement in rocks.*Tectonophysics*,60:89-105.

Gendzwill,D.J. and Stauffer,M.R.,1981.Analysis of triaxial ellipsoids: their shapes, plane sections and plane projections.*Mathematical geology*,13:135-152.

Hayashi,D.,1994.Three dimensional finite strain analysis techniques from strain ellipses on non-parallel sections.*Jour.Geol.Soc.Japan*,100:150-161. (in Japanese with English abstract)

Hayashi,D.,1995.Proposed consistency c-value for strain ellipsoids in geological structure analysis.*Geoinformatics*,6:13-29. (in Japanese with English abstract)

Lisle,R.J.,1977.Clastic grain shape and orientation in relation to cleavage from the Aberystwyth grits, Wales.*Tectonophysics*,39:381-395.

Lisle,R.J.,1985.*Geological strain analysis ; A manual for the method*.Pergamon,Oxford,99pp.

Matthews,P.E.,Bond,R.A.B. and Van Den Berg,J.J.,1974.An algebraic method of strain analysis using elliptical markers.*Tectonophysics*,24:31-67

Milton,N.J.,1980.Determination of the strain ellipsoid from measurements on any three sections.*Tectonophysics*,64:T19-T27.

Oertel,G.,1970.Deformation of a slaty, lapillar tuff in the Lake District, England.*Geol.Soc.Am. Bull.*, 81:1173-1188.

Owens,W.H.,1984.The calculation of a best-fit ellipsoid from elliptical sections on arbitrarily orientated planes.*J.Struct.Geol.*,6:571-578.

Panozzo,R.,1984.Two-dimensional strain from the orientation of lines in a plane.*J.Struct.Geol.*,6:215-221.

Ramsay,J.G.,1967.*Folding and fracturing of rocks*.McGraw-Hill,New York,568pp.

Roberts, B. and Siddans, A. W. B., 1971. Fabric studies in the Llwyd Mawr Ignimbrite, Caernarvonshire, North Wales. *Tectonophysics*, 12:283-306.

Sanderson,D.J.,1977.The analysis of finite strain using lines with an initial random orientation.*Tectonophysics*,43:199-211.

Shimamoto,T. and Ikeda,Y.,1976.A simple algebraic method for strain estimation from deformed ellipsoidal objects.1.Basic theory. *Tectonophysics*,36:315-337.

Woodcock,N.H. and Naylor,M.A.,1983.Randomness testing in three-dimensional orientation data.*J.Struct.Geol.*,5:539-548.